New probe to study the symmetry energy at low nuclear density with the deuteron breakup reaction

Xiao Liang (梁骁),[1] Li Ou (欧立),[1,2,*] and Zhigang Xiao (肖志刚)[3,4,†]
[1]*College of Physics and Technology, Guangxi Normal University, Guilin 541004, China*
[2]*Guangxi Key Laboratory of Nuclear Physics and Technology, Guangxi Normal University, Guilin 541004, China*
[3]*Department of Physics, Tsinghua University, Beijing 100084, China*
[4]*Collaborative Innovation Center of Quantum Matter, Beijing 100084, China*

(Received 21 October 2019; accepted 13 January 2020; published 7 February 2020)

The reactions of nucleons and polarized deuterons scattered off a heavy target nucleus at large impact parameter with intermediate energies have been investigated by using the improved quantum molecular dynamics model. It is found that, due to the opposite effects of isovector potential on protons and neutrons, there is a significant difference between the angle distributions of elastically scattered protons and neutrons. To overcome the lack of a monochromatic neutron beam, the reaction of polarized deuterons peripherally scattered off a heavy target nucleus is used to replace the reaction of individual protons and neutrons scattered off a heavy target nucleus to study the isospin effect. It is found that the distributions of the scattering angle of the proton and the neutron originating from the elastic breakup of the deuteron are very similar to the results of the individual proton- and neutron-induced reactions. A new probe more effective and more clean, namely the difference between the elastic scattering angle of the proton and that of the neutron originating from the breakup of the polarized deuteron, is promoted to constrain the symmetry energy at subsaturation density.

DOI: 10.1103/PhysRevC.101.024603

I. INTRODUCTION

The equation of state (EOS) of isospin asymmetric nuclear matter is still a hot topic nowadays. Especially, the symmetry energy that characterizes the isospin dependence of the EOS has received considerable attention in recent years, because of its importance not only to nuclear physics but also to many issues in astrophysics [1], such as the properties of rare isotopes [2,3]; the stabilities of superheavy nuclei [4]; the dynamics of rare isotope reactions [2,5,6]; the structures, composition, and cooling of neutron stars [7–11]; and the mechanism of core-collapse and the explosion of supernovas [12–14].

Unfortunately, because of the well-known difficulties of treating accurately quantum many-body problems and our poor knowledge about the spin-isospin dependence of many-body forces, theoretical predictions for the density dependence of the symmetry energy [$E_{\rm sym}(\rho)$] of nuclear matter away from the saturation density show large uncertainties [1,15]. Many efforts have been devoted to probing and constraining $E_{\rm sym}(\rho)$ by analyses of terrestrial experiments and astrophysical observations, such as neutron skin [16–19], nuclear mass [20–22], nuclear charge radius [23], the mass-radius relationship [23], α decay [24], giant dipole resonance and pygmy dipole resonance [25–27], isospin diffusion [28–34], isospin drift [35], double neutron to proton ratio [36–43], light-charged particle flow [44–49], the π^-/π^+ ratio [50–54], the K^+/K^0 ratio [55–58], and gravitational waves from merging neutron star binaries [59,60].

Although a general consensus on the constraints of $E_{\rm sym}(\rho)$ at saturation and subsaturation densities [61,62] has been obtained, there is still a considerable uncertainty. Further constraint of $E_{\rm sym}(\rho)$ at subsaturation densities not only is necessary for itself but also is significant for the constraint of $E_{\rm sym}(\rho)$ at suprasaturation densities. It is known that the so-called hadronic observables sensitive to $E_{\rm sym}(\rho)$ at suprasaturation densities in heavy-ion collisions, the π^-/π^+ ratio for example, inevitably suffer from effects of the symmetry energy at low densities during the final state of reaction. Therefore, it is quite important to verify the probed density region of probes. However, one knows these probes are in general sensitive to the high-density or low-density behaviors of the symmetry energy at certain beam energies and impact parameters. Even some established views about the probes face challenge with the deepening of research. For example, some works show that the π^-/π^+ ratio, which is regarded as one of the probes sensitive to $E_{\rm sym}(\rho)$ at suprasaturation densities, however, probes $E_{\rm sym}(\rho)$ around saturation density [63].

The plight of study of the symmetry energy is attributed to two reasons: One is the insufficiency of experimental data, and the other is that the extraction of $E_{\rm sym}(\rho)$ from heavy-ion collisions (HICs) relies unavoidably on transport model simulations in most cases. Although people have organized five international collaborations attempting to find out the origin of different predictions for the same experiments by various transport models and trying to reduce the model uncertainty [64,65], the hope to thoroughly solve the problem is pretty slim for the foreseeable future. It is thus necessary to propose

*liou@gxnu.edu.cn
†xiaozg@tsinghua.edu.cn

more symmetry-energy-sensitive probes, which are effective and free from transport model limitations.

So far, the existing symmetry-energy-sensitive probes are mostly based on HICs. Due to the complexity of HICs, considerable discrepancies in the model outputs lead constraints on $E_{\rm sym}(\rho)$ to be still on the qualitative level. However, some types of direct reaction, like the elastic or quasielastic scattering as well as the direct projectile breakup, involve less degrees of freedom in the reaction process and may reduce the difficulties in modeling the collision. The probes of these kinds of reactions definitely reflect the information of $E_{\rm sym}(\rho)$ at subsaturation densities because the system density is almost unchanged in the reaction process. By properly selecting the range of the impact parameter, one can limit the probed density into narrower windows.

As shown in our previous work, due to the opposite effects of the isovector potential on the proton and the neutron, there is a significant difference in the angle distributions between the proton and the neutron elastically scattered off a heavy target at a large impact parameter [66]. The breakup of the polarized deuteron induced on heavy ions provides a novel and more quantitative constraint to the symmetry energy below half of the saturation density. The correlation angle of the proton and the neutron from the breakup of the deuteron can be a good candidate for a probe for $E_{\rm sym}(\rho)$ at low densities [67]. As a follow-up work, in this article, we promote one more symmetry-energy-sensitive probe, namely the difference between the elastic scattering angle of the proton and that of the neutron originating from the breakup of the deuteron, to constrain $E_{\rm sym}(\rho)$ at low densities.

The article is organized as follows. In Sec. II, we briefly introduce the model. In Sec. III, we present the isospin effect in nucleon-induced reactions and polarized deuteron breakup reactions. Finally a brief summary is given in Sec. IV.

II. MODEL

The improved quantum molecular dynamics (ImQMD) model is an extended version of the quantum molecular dynamics (QMD) model for the simulations of HICs at intermediate beam energies [66,68–70]. The QMD model has been successfully applied in the study of HICs at intermediate energies and also has been applied in proton-induced collisions and provides a consistent description of the experimental data if available [71–75].

In the ImQMD model, each nucleon is described by a Gaussian wave packet,

$$\psi_i(\boldsymbol{r}) = \frac{1}{\left(2\pi\sigma_r^2\right)^{3/4}} \exp\left[-\frac{(\boldsymbol{r}-\boldsymbol{r}_i)^2}{4\sigma_r^2} + \frac{i}{\hbar}\boldsymbol{r}\cdot\boldsymbol{p}_i\right], \tag{1}$$

where $\boldsymbol{r}_i$ and $\boldsymbol{p}_i$ are the center of the ith wave packet in the coordinate space and the momentum space, respectively, and σ_r is the width of wave packet, which satisfies $\sigma_r \cdot \sigma_p = \frac{\hbar}{2}$. By making the Wigner transform on the wave function, the one-body phase-space distribution function can be obtained, which reads as

$$f(\boldsymbol{r},\boldsymbol{p}) = \sum_{i=1}^{A} \frac{1}{(\pi\hbar)^3} \exp\left[-\frac{(\boldsymbol{r}-\boldsymbol{r}_i)^2}{2\sigma_r^2}\right] \exp\left[-\frac{(\boldsymbol{p}-\boldsymbol{p}_i)^2}{2\sigma_p^2}\right]. \tag{2}$$

The time evolution of $\boldsymbol{r}_i$ and $\boldsymbol{p}_i$ for each nucleon is determined by solving the following Hamiltonian equations of motion:

$$\dot{\boldsymbol{r}}_i = \frac{\partial H}{\partial \boldsymbol{p}_i}, \quad \dot{\boldsymbol{p}}_i = -\frac{\partial H}{\partial \boldsymbol{r}_i}, \tag{3}$$

where

$$H = T + U_{\rm Coul} + U_{\rm loc}. \tag{4}$$

Here, the kinetic energy $T = \sum_i \frac{p_i^2}{2m}$, $U_{\rm Coul}$ is the Coulomb energy, and the nuclear local potential energy $U_{\rm loc} = \int V_{\rm loc}[\rho(\boldsymbol{r})]d\boldsymbol{r}$, where $V_{\rm loc}$ is the full Skyrme-type potential energy density functional with just the spin-orbit term omitted, which reads

$$\begin{aligned} V_{\rm loc} =& \frac{\alpha}{2}\frac{\rho^2}{\rho_0} + \frac{\beta}{\eta+1}\frac{\rho^{\eta+1}}{\rho_0^{\eta}} + \frac{g_{\rm sur}}{2\rho_0}(\nabla\rho)^2 + \frac{g_{\rm sur,iso}}{\rho_0}[\nabla(\rho_n-\rho_p)]^2 \\ &+ g_{\rho\tau}\frac{\rho^{8/3}}{\rho_0^{5/3}} + (A\rho + B\rho^{\gamma} + C\rho^{5/3})\delta^2\rho, \end{aligned} \tag{5}$$

where ρ_0, ρ, ρ_n, and ρ_p are the saturation density, the nucleon density, the neutron density, and the proton density, respectively, and the isospin asymmetry degree $\delta = (\rho_n - \rho_p)/(\rho_n + \rho_p)$. All the parameters in Eq. (5) can be derived from the standard Skyrme interaction parameters [66]. To mimic the strong variation of $E_{\rm sym}(\rho)$ as well as keep the isoscalar part of EOS unchanged, the volume symmetry potential energy term [corresponding to the last term in Eq. (5)] is replaced with the form of $\frac{C_{\rm s,p}}{2}(\frac{\rho}{\rho_0})^{\gamma}\rho$, by setting $A_{\rm sym} = C_{\rm sym} = 0$ and $B_{\rm sym} = \frac{C_{\rm s,p}}{2}$. Then the symmetry energy is written as

$$E_{\rm sym}(\rho) = \frac{C_{\rm s,k}}{2}\left(\frac{\rho}{\rho_0}\right)^{2/3} + \frac{C_{\rm s,p}}{2}\left(\frac{\rho}{\rho_0}\right)^{\gamma}, \tag{6}$$

where $C_{\rm s,k}$ and $C_{\rm s,p}$ are the symmetry kinetic and potential energy parameters, respectively. The Skyrme parameter set MSL0 [17], one of Skyrme parameter sets which best satisfy the current understanding of the physics of nuclear matter over a wide range of applications [76], is used in this work. By using various γ, one can get MSL0-like Skyrme interactions with various $E_{\rm sym}(\rho)$. In Fig. 1, we present the density dependence of the symmetry energy given by MSL0-like Skyrme interactions with $\gamma = 0.5$, 1.0, and 2.0 adopted. The boxes in Fig. 1 indicate the probed density windows of observables in the reactions with the impact parameters $b = 6$, 7, and 8 fm, which is discussed in the following text. The impact parameter b, as shown in Fig. 2, is defined as the perpendicular distance between the initial vector velocity of a projectile and the center of target that the projectile is approaching.

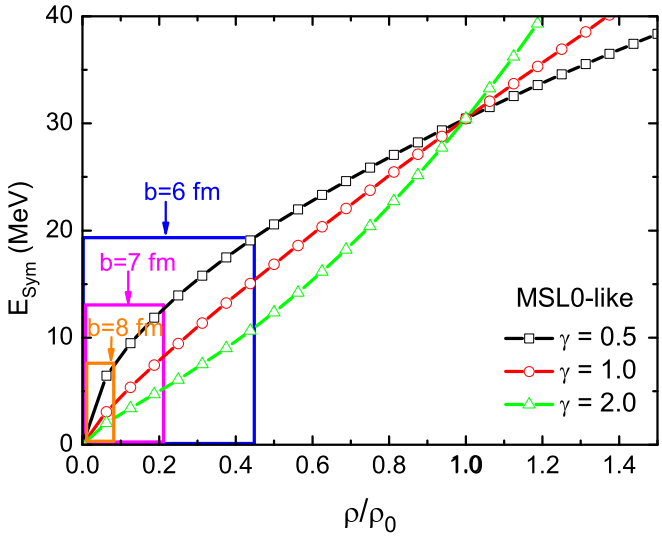

FIG. 1. The density dependence of the symmetry energy given by MSL0-like Skyrme interactions with $\gamma = 0.5$, 1.0, and 2.0 adopted.

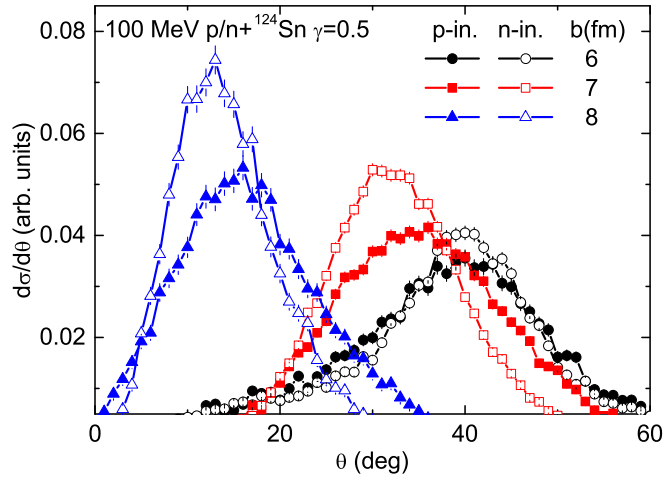

FIG. 3. The angular distributions of elastically scattered protons and neutrons in nucleon-induced reactions on ^{124}Sn at $E = 100$ MeV and $b = 6$, 7, and 8 fm.

While the initialization of the heavy ion is done as usual as described in Ref. [69], the deuteron is semiclassically initialized in a simplified scheme as follows. The neutron-to-proton direction is taken as the long symmetric axis (LSA). The initial distance between the neutron and the proton is set to $3 \pm \Delta r$ fm, where Δr is a random value in the range of 0–0.25 fm. The spatial coordinates and the momentum coordinates perpendicular to the LSA are set to zero. The direction of the momentum is initially set to be opposed for the neutron and the proton along the LSA, and the initial magnitude of the momentum is sampled randomly to obtain a stable deuteron until 100 fm/c, namely the root-mean-square radius of the deuteron remains at 2.1 ± 0.5 fm, where 2.1 fm is the experimental value for the root-mean-square radius of the deuteron [77]. By rotating the LSA randomly or in a certain direction, one can mimic the unpolarized or preoriented deuteron beam as the initial state, respectively. For this simplification, the initial distance between the mass centers of projectile and the target is set to 25 fm. Then, the deuteron will soon enter the target potential field in 30 fm/c for reactions with a beam energy of 100 MeV/u.

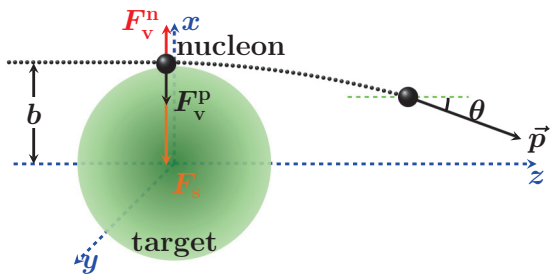

FIG. 2. The schematic view of a nucleon peripherally scattered off of a heavy target.

III. RESULTS AND DISCUSSIONS

In this section, we illustrate and discuss the dynamical isospin effects in nucleon-induced reactions and deuteron-induced reactions.

A. Isospin effects in nucleon-induced reactions

When a nucleon peripherally passes by a heavy target nucleus, as shown by the illustration in Fig. 2, the nucleon experiences the nuclear force and the proton experiences the Coulomb force F_c. While the isoscalar nuclear force F_s is attractive to both the proton and the neutron, the isovector force F_v is attractive to the proton and repulsive to the neutron in the subsaturation density environment. This dynamical isospin effect should have the opposite effect on the elastic scattering angles of protons and neutrons and leads to the disparity between the angular distributions of the elastic scattering of protons and neutrons for the same incident energy and initial geometry.

This conjecture has already been verified in our previous work; see Ref. [66] for details. The angular distributions of the elastic scattering of protons and neutrons in the proton- or neutron-induced reaction on ^{124}Sn at $E = 100$ MeV and $b = 6$, 7, and 8 fm with the same symmetry energy parameter $\gamma = 0.5$ adopted in the calculations are shown in Fig. 3. One can see clearly that the nucleon-emitting angle decreases as b increases because the attraction from the target nucleus becomes weaker. For the cases of $b = 7$ and 8 fm, the elastically scattered protons show a trend to emit into a larger angle while the elastically scattered neutrons show a trend to emit into a smaller angle. For the case of $b = 6$ fm, the difference fades away due to the strong isoscalar potential dominating the scattering and smears the isovector potential effect on the proton or the neutron.

Naturally, $E_{sym}(\rho)$ will affect the elastic scattering angle of the incident nucleon. For example, the angular distributions of emitted nucleons with two forms of $E_{sym}(\rho)$ ($\gamma = 0.5$ and 2.0) adopted are shown in Fig. 4.

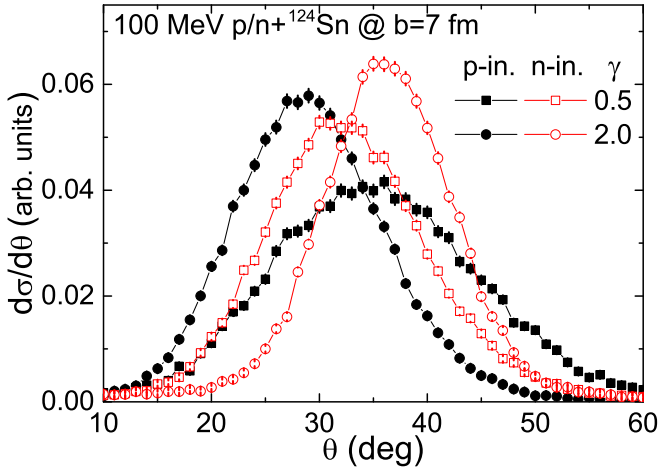

FIG. 4. The angular distributions of elastically scattered protons and neutrons in nucleon-induced reactions on ^{124}Sn at $E = 100$ MeV and $b = 7$ fm calculated with $\gamma = 0.5$ and 2.0.

With the form of the power function, the symmetry potential with $\gamma = 2.0$ is weaker than that with $\gamma = 0.5$ at subsaturation densities. So the peak of the proton distribution with $\gamma = 2.0$ shifts to a smaller angle because the attraction from the isovector potential on the proton becomes weaker. While the peak of the neutron distribution with $\gamma = 2.0$ shifts to a larger angle because the repulsion from the isovector potential on the neutron becomes weaker.

The angular distributions of emitted nucleons with various $E_{\rm sym}(\rho)$ ($\gamma = 0.5$–2.0) adopted are shown in Fig. 5. One can see that there are regular relations between the angle distributions and the stiffnesses of the symmetry energy, except in the case of $b = 6$ fm. The peak of the proton distribution shows a trend to locate at a larger angle with a smaller γ value, while the peak of the neutron distribution shows a trend to locate at a smaller angle with a smaller γ value. To quantify the angle distribution in connection with the stiffness of the symmetry energy, the angle distributions are fitted with Gaussian distribution functions of θ as

$$\sigma = \sigma_0 + \frac{A}{W\sqrt{\pi/2}} e^{-2\frac{(\theta-\theta_c)^2}{W^2}}, \tag{7}$$

which are presented in Fig. 5 by the corresponding curves.

Then the locations of peaks of distributions θ_c and the widths of distributions W as a function of γ, as shown in Fig. 6, can be used to study $E_{\rm sym}(\rho)$. To scale the effect of the symmetry energy on the observable, when γ changes from 0.5 to 2.0, the relative variation of the observable is defined as

$$R = \frac{|y(0.5) - y(2.0)|}{\min[|y(0.5)|, |y(2.0)|]} 100\%. \tag{8}$$

One can see that, as the symmetry energy becomes stiffer, the locations of peaks of distribution of protons θ_c^p become smaller, except in the case of $b = 6$ fm, which is not sensitive to the symmetry energy. In the case of $b = 7$ fm, the effect of the symmetry energy is about 21%. The locations of peaks of distribution of neutrons θ_c^n become larger as the symmetry energy becomes stiffer; the effect of the symmetry energy is about 12%.

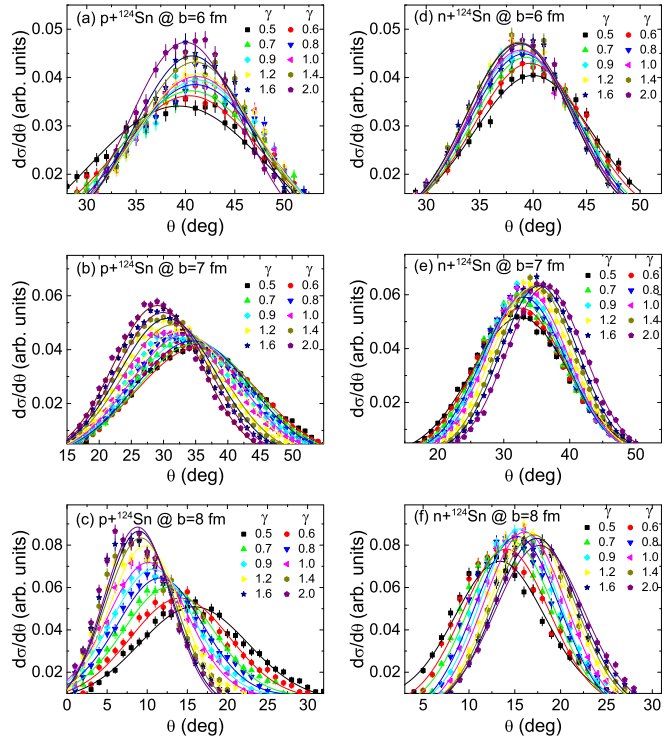

FIG. 5. The angular distributions of elastically scattered protons (left panels) and neutrons (right panels) in corresponding nucleon-induced reactions on ^{124}Sn at $E = 100$ MeV and $b = 6$ fm [panels (a) and (d)], $b = 7$ fm [panels (b) and (e)], and $b = 8$ fm [panels (c) and (f)] with various $E_{\rm sym}(\rho)$ values adopted in the calculations. The curves are the results of fitting the calculations with Gaussian functions.

As the symmetry energy becomes stiffer, the widths of distributions for both protons and neutrons become smaller; the effects of the symmetry energy are about 38% and 25%,

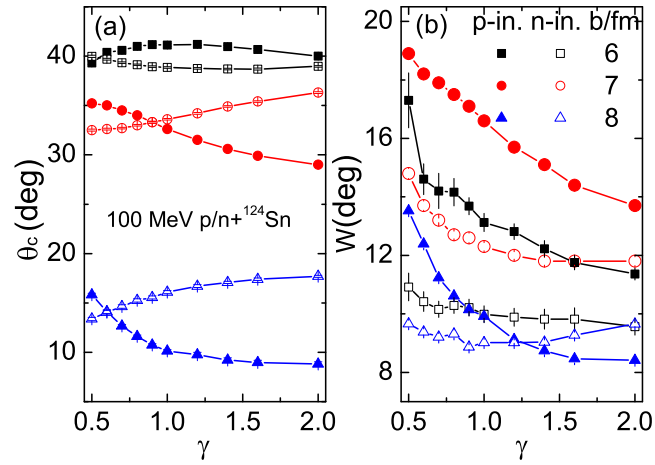

FIG. 6. The γ dependencies of the locations of peaks of distributions θ_c (a) and the widths of distributions W (b) for protons and neutrons elastically scattered off of ^{124}Sn at $E = 100$ MeV and $b = 7$ fm.

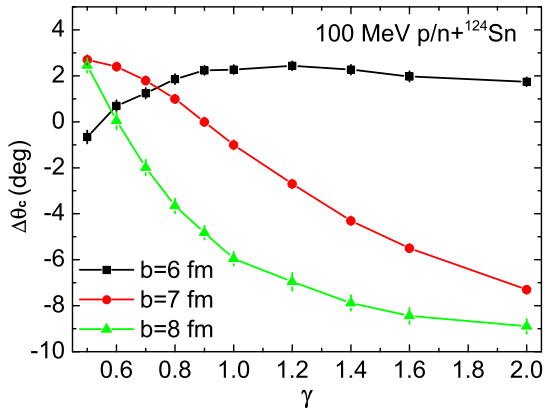

FIG. 7. The γ dependencies of the difference between the locations of peaks of distributions of elastically scattered protons and neutrons in the corresponding nucleon elastically scattered off of ^{124}Sn at $E = 100$ MeV and $b = 6$, 7, and 8 fm.

respectively. The sensitivities of these observables are close to those of existing observables with sensitivities of about 20%. To get a more sensitive observable, the difference between the locations of peaks of distributions of protons and neutrons, namely $\Delta\theta_c = \theta_c^p - \theta_c^n$, can be constructed. The γ dependence of $\Delta\theta_c$ is presented in Fig. 7. One can see that, as the symmetry energy becomes stiffer, $\Delta\theta_c$ changes from positive to negative, and the sensitivity of $\Delta\theta_c$ to γ is about 370% for $b = 7$ fm, which is more highly sensitive than the existing observables.

B. Isospin effects in deuteron-induced reactions

Because monochromatic neutron beams with high energy are hardly available, conducting experiments for neutron-induced reactions remains a difficult task. Thanks to the availability of polarized deuteron beams at hundreds of MeV/u at various running accelerators around the world [78–82], the deuteron, with one proton and one neutron bound loosely at a large average separation distance, provides an alternative opportunity to execute "proton- and neutron-induced" reactions by deuteron-induced reactions. If a deuteron breaks without collision when it peripherally passes by a heavy target nucleus, it provides a mixed proton-neutron beam to probe the isospin effect. As shown by the illustration in Fig. 8,

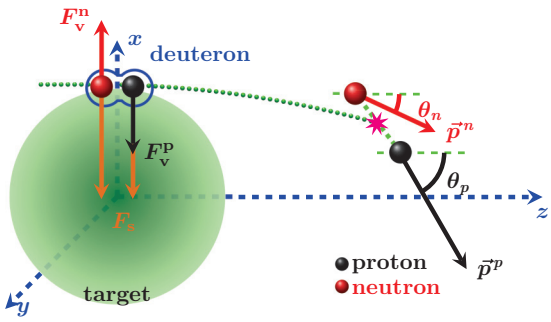

FIG. 8. The schematic view of a deuteron-induced peripheral collision on a heavy target nucleus.

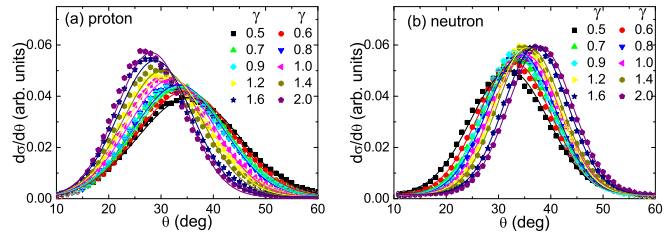

FIG. 9. The angle distributions of protons (a) and neutrons (b) from the breakup of deuterons elastically scattered off of ^{124}Sn with 100 MeV/u and $b = 7$ fm.

the two nucleons in the deuteron experience nuclear force and Coulomb force F_c, and the latter is repulsive only for protons. While the isoscalar nuclear force F_s is attractive to both nucleons, the isovector force F_v is attractive to protons and repulsive to neutrons.

Because of the exchange symmetry of the wave function with the exchange of n and p, as done in Ref. [67], the simulation is done by mimicking a fully tensor- and vector-polarized deuteron beam with a 50% possibility for $\vec{r}^{\,np}//\vec{k}$ and a 50% possibility for $-\vec{r}^{\,np}//\vec{k}$, where $\vec{r}^{\,np}$ is the relative vector from neutron to proton and $\vec{k}$ is the particle wave vector. In the following calculations, the LSA of the deuteron is preorientated parallel to the beam axis.

The angle distributions of protons and neutrons from the breakup of polarization deuterons elastically scattered off of ^{124}Sn with 100 MeV/u and $b = 7$ fm are shown in Fig. 9.

One can see that the behaviors of the angle distributions of elastically scattered protons and neutrons originating from the breakup of deuterons are quite similar to those in nucleon-induced reactions. The softer symmetry energy gives a wider distribution, a larger local angle of the peak for proton distribution, and a smaller local angle of the peak for neutron distribution. For more clear and direct comparison, the corresponding nucleon angular distributions for the free nucleon-induced and the deuteron-induced reactions for $b = 7$ and 8 fm with $\gamma = 0.5$, 1.0, and 2.0 are presented in Fig. 10. One can see that the corresponding distributions are similar to each other, with only tiny differences.

Once again, the angle distributions are fitted with Gaussian distribution functions, and the γ dependencies of the location of peaks θ_c and widths W of distributions are shown in Fig. 11. The locations of peaks θ_c and widths W of distributions for deuteron-induced reactions are very close to those

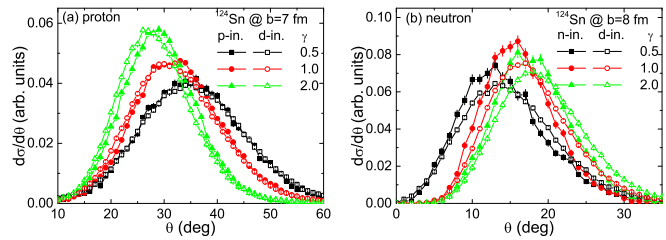

FIG. 10. The angle distributions of protons and neutrons from the breakup of deuterons elastically scattered off of ^{124}Sn with 100 MeV/u and $b = 7$ and 8 fm, compared with those from corresponding nucleon-induced reactions.

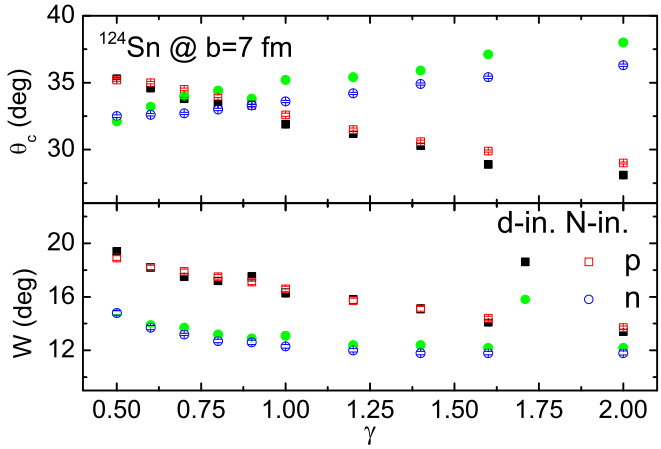

FIG. 11. The γ dependencies of the location of peaks θ_c and widths W of distributions of elastically scattered protons and neutrons, where "d-in." denotes $E = 100$ MeV/u deuteron-induced reactions and "N-in." denotes $E = 100$ MeV proton- or neutron-induced reactions on ^{124}Sn at $b = 7$ fm.

for nucleon-induced reactions. This means that the protons and neutrons from the breakup of deuterons in polarized deuteron-induced reactions indeed play "synchronously" the corresponding role of nucleon projectiles in nucleon-induced reactions.

Therefore, one can use the difference between the scattering angle of the proton and the neutron ($\delta\theta = \theta_p - \theta_n$) from the breakup of the deuteron in each single event, but not the difference between the locations of peaks of distributions of protons and neutrons, to study $E_{\rm sym}(\rho)$. By this method, the influence from the uncertainty of the isoscalar potential can be further reduced, because the proton and the neutron from the breakup of the deuteron in the same event undergo nearly the same isoscalar potential from the target. In Fig. 12, γ dependencies of $\delta\theta$ distributions in $E = 100$ MeV/u deuteron-induced reactions on ^{124}Sn at $b = 6$, 7, 8, and 6.5–8.5 fm are

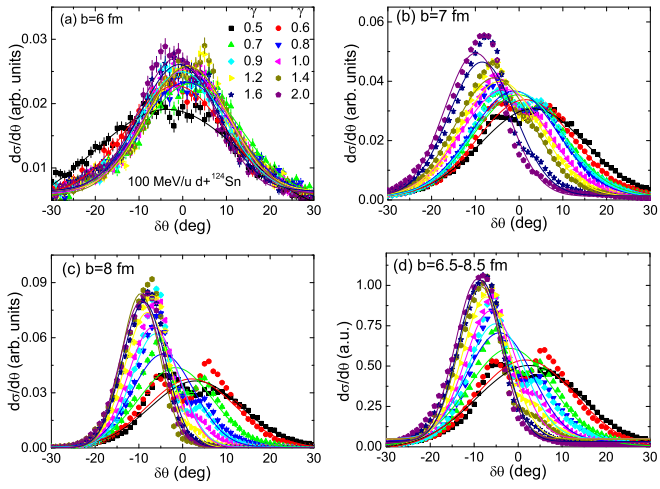

FIG. 12. The γ dependencies of the difference between the elastic scattering angles of protons and neutrons originating from the breakup of deuterons in deuteron-induced reactions on ^{124}Sn with $E = 100$ MeV/u at $b = 6$, 7, 8, and 6.5–8.5 fm.

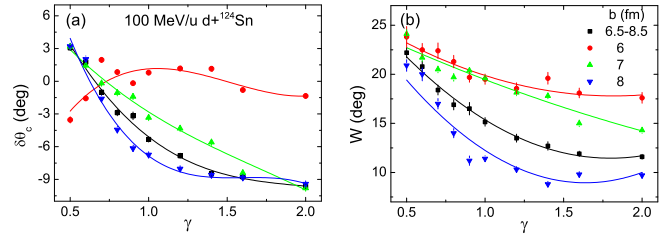

FIG. 13. The γ dependencies of the locations of peaks (a) and widths (b) of distributions of differences between the elastic scattering angles of protons and neutrons originating from the breakup of deuterons in deuteron-induced reactions on ^{124}Sn with $E = 100$ MeV/u at $b = 6$, 7, 8, and 6.5–8.5 fm.

presented. For the case of $b = 6$ fm, in which the deuteron is very close to the target, the isoscalar potential dominates the scattering, the distinctions between the distributions with various $E_{\rm sym}(\rho)$ are not obvious, all centers of $\delta\theta$ distributions locate around zero degrees, and the widths of the distributions are almost the same. As the impact parameter increases, the isovector potential effect becomes obvious. The distribution with the soft symmetry energy is wider than that with the stiff one. The centers of $\delta\theta$ distributions with the soft symmetry energy show a trend to locate at positive angles relative to those with the stiff one, which show a trend to locate at negative angles. From the results of $b = 7$ and 8 fm, the $\delta\theta$ distribution is not too sensitive to the fine division of the impact parameter. That is very helpful to eliminate much of the hardship in experiments and to improve the accuracy of constraint on $E_{\rm sym}(\rho)$. Because the impact parameter is not a directly measurable quantity, usually the impact parameter range is estimated through various means (see Ref. [83] for more details). Here we also give the results of peripheral reactions with the parameter range $b = 6.5$–8.5 fm. Finally one can see that the results in peripheral collisions mixed with $b = 6.8$–8.5 fm still exhibit sensitivity to $E_{\rm sym}(\rho)$. One thing worth mentioning is that there are two peaks of distribution for the rather soft $E_{\rm sym}(\rho)$ (small γ). That is because the tensor- and vector-polarized deuteron beam contains a 50% possibility for $\vec{r}^{\,np}//\vec{k}$ and a 50% possibility for $-\vec{r}^{\,np}//\vec{k}$. The stronger isovector force forms a torque acting on the proton and the neutron and modifies the orientation of the incident deuteron before the breakup [67].

Fitting all distributions with Gaussian functions, one can get the locations of peaks and widths of $\delta\theta$ distributions. The γ dependencies of the locations of peaks and widths are presented in Fig. 13. From the results, one can find the following: For small impact parameters, i.e., $b = 6$ fm, $\delta\theta_c$ is not sensitive to γ. For large impact parameters, $\delta\theta_c$ shows strong sensitivity to $E_{\rm sym}(\rho)$, decreasing from positive to negative degrees with increasing stiffness of the symmetry energy. Moreover, the widths of the distributions W show sensitivity to γ for all impact parameters. Again we give the results of peripheral reactions with the parameter range $b = 6.5$–8.5 fm. One can see that the effects of the symmetry energy on $\delta\theta_c$ and W are about 415% and 95%, respectively. Although $\delta\theta_c$ and W are not so sensitive in the case of $\gamma > 1.2$, this does not impede $\delta\theta_c$ and W from being good candidates to probe

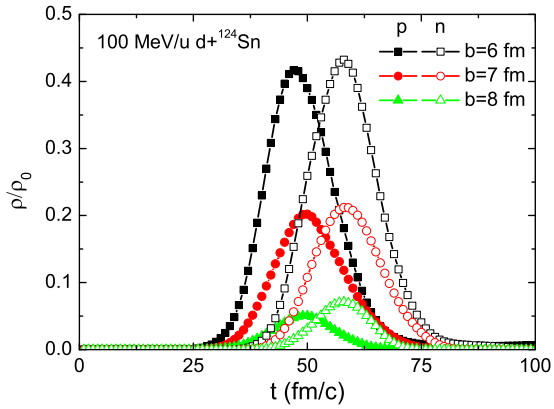

FIG. 14. The local densities experienced by protons and neutrons from the breakup of deuterons elastically scattered off of ^{124}Sn with 100 MeV/u with various impact parameters as functions of time.

$E_{\rm sym}(\rho)$, because the very stiff symmetry energy with $\gamma > 1.5$ has been ruled out by existing experiments and theories.

Finally, the probed density of this method should be indicated clearly. In Fig. 14, the local density experienced by protons and neutrons from the breakup of deuterons elastically scattered off of ^{124}Sn with 100 MeV/u with various impact parameters as functions of time are presented. One can see clearly that the elastically scattering protons and neutrons in deuteron peripheral reactions pass through the periphery of the target nuclei where the density is below half of the saturation density. The $E_{\rm sym}(\rho)$ windows probed by this method are shown in Fig. 1 by boxes for various impact parameters. It is reasonable to assert that the upper limit of the $E_{\rm sym}(\rho)$ window is below $0.3\rho_0$, because for the case of $b = 6$ fm most of the collisions (about 94%) are inelastic scattering due to collisions with targets.

IV. SUMMARY

Within the ImQMD model, proton-induced and neutron-induced reactions on heavy target nuclei with 100-MeV incident energies have been studied. It is found that, due to the isovector potential, there is a significant difference between the elastic scattering angles of protons and neutrons in peripheral reactions. The difference between the locations of peaks of distributions of protons or neutrons elastically scattered off of heavy targets is very sensitive to the density dependence of the symmetry energy. To overcome the lack of a monochromatic neutron beam, the polarized deuteron peripherally scattered off of a heavy target nucleus has been investigated. It is found that the behaviors of angle distribution of elastic-scattering protons and neutrons originating from the breakup of deuterons are quite similar to those in corresponding nucleon-induced reactions. Therefore, the polarized deuteron scattered off of a heavy target nucleus can be an alternative to the individual proton- and neutron-induced reactions. In terms of the sensitivity and the cleanness, a new probe, namely the difference between the elastic scattering angle of the proton and that of the neutron originating from the breakup of the deuteron, is promoted to be a promising candidate to constrain the symmetry energy at subsaturation densities.

ACKNOWLEDGMENTS

This work has been supported by the National Natural Science Foundation of China under Grants No. 11965004, No. 11875174, No. 11890712, No. U1867212, No. 11711540016, and No. 11847317; the Natural Science Foundation of Guangxi Province under Grants No. 2016GXNSFFA380001 and No. 2017GXNSFGA198001; the Foundation of Guangxi Innovative Team and Distinguished Scholar in Institutions of Higher Education, and the Tsinghua University Initiative Scientific Research Program.

[1] B. A. Li, L. W. Chen, and C. M. Ko, Phys. Rep. **464**, 113 (2008).
[2] V. Baran, M. Colonna, V. Greco, and M. Di Toro, Phys. Rep. **410**, 335 (2005).
[3] N. Nikolov, N. Schunck, W. Nazarewicz, M. Bender, and J. Pei, Phys. Rev. C **83**, 034305 (2011).
[4] J. Dong, W. Zuo, and W. Scheid, Phys. Rev. Lett. **107**, 012501 (2011).
[5] A. W. Steiner, M. Prakash, J. Lattimer, and P. J. Ellis, Phys. Rep. **411**, 325 (2005).
[6] J. M. Lattimer and M. Prakash, Phys. Rep. **442**, 109 (2007).
[7] J. M. Lattimer and M. Prakash, Phys. Rep. **333**, 121 (2000).
[8] C. J. Horowitz and J. Piekarewicz, Phys. Rev. Lett. **86**, 5647 (2001).
[9] B. G. Todd-Rutel and J. Piekarewicz, Phys. Rev. Lett. **95**, 122501 (2005).
[10] B. K. Sharma and S. Pal, Phys. Lett. B **682**, 23 (2009).
[11] M. Prakash, T. L. Ainsworth, and J. M. Lattimer, Phys. Rev. Lett. **61**, 2518 (1988).
[12] P. Bonche and D. Vautherin, Nucl. Phys. A **372**, 496 (1981).
[13] G. Watanabe, H. Sonoda, T. Maruyama, K. Sato, K. Yasuoka, and T. Ebisuzaki, Phys. Rev. Lett. **103**, 121101 (2009).
[14] G. Shen, C. J. Horowitz, and S. Teige, Phys. Rev. C **83**, 035802 (2011).
[15] B. A. Brown, Phys. Rev. Lett. **85**, 5296 (2000).
[16] M. Warda, X. Vinas, X. Roca-Maza, and M. Centelles, Phys. Rev. C **81**, 054309 (2010).
[17] L.-W. Chen, C.-M. Ko, B.-A. Li, and J. Xu, Phys. Rev. C **82**, 024321 (2010).
[18] M. K. Gaidarov, A. N. Antonov, P. Sarriguren, and E. M. de Guerra, Phys. Rev. C **85**, 064319 (2012).
[19] L. Min, L. Zhu-Xia, W. Ning, and Z. Feng-Shou, Chin. Phys. C **35**, 629 (2011).
[20] N. Wang, L. Ou, and M. Liu, Phys. Rev. C **87**, 034327 (2013).
[21] X. Fan, J. Dong, and W. Zuo, Phys. Rev. C **89**, 017305 (2014).
[22] P. Danielewicz and J. Lee, Nucl. Phys. A **818**, 36 (2009).
[23] N. Wang and T. Li, Phys. Rev. C **88**, 011301(R) (2013).
[24] J. Dong, W. Zuo, and J. Gu, Phys. Rev. C **87**, 014303 (2013).
[25] A. Carbone, G. Colò, A. Bracco, L.-G. Cao, P. F. Bortignon, F. Camera, and O. Wieland, Phys. Rev. C **81**, 041301(R) (2010).
[26] O. Wieland, A. Bracco, F. Camera *et al.*, Phys. Rev. Lett. **102**, 092502 (2009).

[27] J. Piekarewicz, Phys. Rev. C **83**, 034319 (2011).
[28] M. B. Tsang, W. A. Friedman, C. K. Gelbke, W. G. Lynch, G. Verde, and H. S. Xu, Phys. Rev. Lett. **86**, 5023 (2001).
[29] H.-Y Wu, Z.-G Xiao, G.-M Jin *et al.*, Phys. Lett. B **538**, 39 (2002).
[30] M. B. Tsang, T. X. Liu, L. Shi *et al.*, Phys. Rev. Lett. **92**, 062701 (2004).
[31] L. W. Chen, C. M. Ko, and B.-A. Li, Phys. Rev. Lett. **94**, 032701 (2005).
[32] T. X. Liu, W. G. Lynch, M. B. Tsang *et al.*, Phys. Rev. C **76**, 034603 (2007).
[33] Z. Y. Sun, M. B. Tsang, W. G. Lynch, G. Verde, F. Amorini, L. Andronenko, M. Andronenko, G. Cardella, M. Chatterje, P. Danielewicz *et al.*, Phys. Rev. C **82**, 051603(R) (2010).
[34] J. Rizzo, M. Colonna, V. Baran, M. Di Toro, H. H. Wolter, and M. Zielinska-Pfabe, Nucl. Phys. A **806**, 79 (2008).
[35] Y. Zhang, J. Tian, W. Cheng *et al.*, Phys. Rev. C **95**, 041602(R) (2017).
[36] B. A. Li, L. W. Chen, G. C. Yong, and W. Zuo, Phys. Lett. B **634**, 378 (2006).
[37] M. A. Famiano, T. Liu, W. G. Lynch *et al.*, Phys. Rev. Lett. **97**, 052701 (2006).
[38] Y. Zhang, P. Danielewicz, M. Famiano, Z. Li, W. G. Lynch, and M. B. Tsang, Phys. Lett. B **664**, 145 (2008).
[39] M. B. Tsang, Y. Zhang, P. Danielewicz, M. Famiano, Z. Li, W. G. Lynch, and A. W. Steiner, Phys. Rev. Lett. **102**, 122701 (2009).
[40] S. Kumar, Y. G. Ma, G. Q. Zhang, and C. L. Zhou, Phys. Rev. C **84**, 044620 (2011).
[41] Y. Zhang, D. D. S. Coupland, P. Danielewicz, Z. X. Li, H. Liu, F. Lu, W. G. Lynch, and M. B. Tsang, Phys. Rev. C **85**, 024602 (2012).
[42] Y. X. Zhang, M. B. Tsang, Z. X. Li, and H. Liu, Phys. Lett. B **732**, 186 (2014).
[43] Wen.-J. Xie, Jun. Su, L. Zhu, and F.-S. Zhang, Phys. Rev. C **88**, 061601(R) (2013).
[44] J. Rizzo, M. Colonna, M. Di Toro, and V. Greco, Nucl. Phys. A **732**, 202 (2004).
[45] G.-C. Yong, B.-A. Li, L.-W. Chen, and X.-C. Zhang, Phys. Rev. C **80**, 044608 (2009).
[46] Z. Kohley, L. W. May, S. Wuenschel *et al.*, Phys. Rev. C **82**, 064601 (2010).
[47] V. Giordano, M. Colonna, M. Di Toro, V. Greco, and J. Rizzo, Phys. Rev. C **81**, 044611 (2010).
[48] M. D. Cozma, Phys. Lett. B **700**, 139 (2011).
[49] Y. Wang, C. Guo, Q. Li, H. Zhang, Y. Leifels, and W. Trautmann, Phys. Rev. C **89**, 044603 (2014).
[50] Z. Xiao, B.-A. Li, L.-W. Chen, G.-C. Yong, and M. Zhang, Phys. Rev. Lett. **102**, 062502 (2009).
[51] Z.-Q. Feng and G.-M. Jin, Phys. Lett. B **683**, 140 (2010).
[52] Y. Gao, G. C. Yong, Y. Wang, Q. Li, and W. Zuo, Phys. Rev. C **88**, 057601 (2013).
[53] J. Hong and P. Danielewicz, Phys. Rev. C **90**, 024605 (2014).
[54] Z.-G. Xiao, G.-C. Yong, L.-W. Chen *et al.*, Eur. Phys. J. A **50**, 37 (2014).
[55] X. Lopez, Y. J. Kim *et al.*, Phys. Rev. C **75**, 011901(R) (2007).
[56] Q. Li, Z. Li, S. Soff *et al.*, J. Phys. G: Nucl. Part. Phys. **31**, 1359 (2005).
[57] G. Ferini, T. Gaitanos, M. Colonna, M. Di Toro, and H. H. Wolter, Phys. Rev. Lett. **97**, 202301 (2006).
[58] Z.-Q. Feng, Phys. Rev. C **87**, 064605 (2013).
[59] A. W. Steiner and S. Gandolfi, Phys. Rev. Lett. **108**, 081102 (2012).
[60] K. Takami, L. Rezzolla, and L. Baiotti, Phys. Rev. Lett. **113**, 091104 (2014).
[61] M. B. Tsang, J. R. Stone, F. Camera *et al.*, Phys. Rev. C **86**, 015803 (2012).
[62] J. M. Lattimer and A. W. Steiner, Eur. Phys. J. A **50**, 40 (2014).
[63] G.-C. Yong, Y. Gao, G.-F. Wei, Y.-F. Guo, and W. Zuo, J. Phys. G: Nucl. Part. Phys. **46**, 105105 (2019).
[64] Y.-X. Zhang, Y.-J. Wang, M. Colonna *et al.*, Phys. Rev. C **97**, 034625 (2018).
[65] J. Xu *et al.*, Phys. Rev. C **93**, 044609 (2016).
[66] L. Ou, Z. Li, and X. Wu, Phys. Rev. C **78**, 044609 (2008).
[67] L. Ou, Z. Xiao, H. Yi *et al.*, Phys. Rev. Lett. **115**, 212501 (2015).
[68] J. Aichelin, Phys. Rep. **202**, 233 (1991).
[69] N. Wang, Z. Li, and X. Wu, Phys. Rev. C **65**, 064608 (2002).
[70] Y. Zhang and Z. Li, Phys. Rev. C **71**, 024604 (2005).
[71] K. Niita, S. Chiba, T. Maruyama, T. Maruyama, H. Takada, T. Fukahori, Y. Nakahara, and A. Iwamoto, Phys. Rev. C **52**, 2620 (1995).
[72] S. Chiba, M. B. Chadwick, K. Niita, T. Maruyama, T. Maruyama, and A. Iwamoto, Phys. Rev. C **53**, 1824 (1996).
[73] S. Chiba, O. Iwamoto, T. Fukahori, K. Niita, T. Maruyama, T. Maruyama, and A. Iwamoto, Phys. Rev. C **54**, 285 (1996).
[74] L. Ou, Y. Zhang, J. Tian, and Z. Li, J. Phys. G: Nucl. Part. Phys. **34**, 827 (2007).
[75] L. Ou, Z. Li, X. Wu *et al.*, J. Phys. G: Nucl. Part. Phys. **36**, 125104 (2009).
[76] M. Dutra, O. Lourenço, J. S. Sá Martins, A. Delfino, J. R. Stone, and P. D. Stevenson, Phys. Rev. C **85**, 035201 (2012).
[77] I. Sick and D. Trautmann, Phys. Lett. B **375**, 16 (1996).
[78] W. Lakin, Phys. Rev. **98**, 139 (1955).
[79] V. S. Morozov, Z. B. Etienne, M. C. Kandes, A. D. Krisch, M. A. Leonova, D. W. Sivers, V. K. Wong, K. Yonehara, V. A. Anferov, H. O. Meyer, P. Schwandt, E. J. Stephenson, and B. von Przewoski, Phys. Rev. Lett. **91**, 214801 (2003).
[80] V. S. Morozov, A. W. Chao, A. D. Krisch, M. A. Leonova, R. S. Raymond, D. W. Sivers, V. K. Wong, and A. M. Kondratenko, Phys. Rev. Lett. **103**, 144801 (2009).
[81] K. Hatanaka, K. Takahisa, H. Tamura, M. Sato, and I. Miura, Nucl. Instrum. Methods Phys Res., Sect. A **384**, 575 (1997).
[82] H. Okamura, H. Sakai, N. Sakamoto *et al.*, AIP Conf. Proc. **293**, 84 (1993).
[83] L. Li, Y. Zhang, Z. Li, N. Wang, Y. Cui, and J. Winkelbauer, Phys. Rev. C **97**, 044606 (2018).